3D1-2

Acceleration of FGMRES Using Fast Multipole Method for Method of Moments Based on Combined Tangential Formulation

Hidetoshi Chiba [1], Toru Fukasawa [1], Hiroaki Miyashita [1], and Yoshihiko Konishi [1]
[1] Mitsubishi Electric Corporation
5-1-1 Ofuna, Kamakura, Kanagawa, 247-8501 Japan, Chiba.Hidetoshi@eb.MitsubishiElectric.co.jp

1. Introduction

In this study, we demonstrate an acceleration of flexible generalized minimal residual algorithm (FGMRES)[1] implemented with the method of moments and the fast multipole method (FMM), based on a combined tangential formulation. For the implementation of the FGMRES incorporated with the FMM concept, we propose a new definition of the truncation number for the FMM operator within the inner solver. The proposed truncation number provides an optimal variable preconditioner by controlling the accuracy and computational cost of the inner iteration.

2. FGMRES Implemented with the FMM

The conceptual diagram of the inner-outer FGMRES methods implemented with the FMM techniques is shown in Figure 1. We define the truncation number $L^i_{m,l}$ for the l-th MLFMA level and medium m as follows:

$$L^i_{m,l} = \min\left(\left\lfloor r_1 L^o_{m,1} \left(\frac{a_l}{a_1} \right)^p \right\rfloor, \left\lfloor r_2 L^o_{m,l} \right\rfloor \right), \tag{1}$$

where, p denotes the rate of increase of the truncation number corresponding to the MLFMA level and a smaller l indicates a finer (lower) MLFMA level. In Eq. (1), $\lfloor \cdot \rfloor$ stands for the floor operation, a_l indicates the cluster size of the l-th MLFMA level, the parameters r_1 and r_2 are real numbers in the range [0, 1], and $L^o_{m,l}$ represents the truncation number of the l-th MLFMA level and medium m for the outer solver. r_2 represents the ratio of the truncation number of the inner solver to that of the outer solver. Hence, r_2 ensures that $L^i_{m,l}$ is less than $L^o_{m,l}$ multiplied by r_2, regardless of the settings for r_1 and p. Using r_2 and the $\min(\cdot)$ operation, we can always keep the FMM operator for the inner solver less accurate and cheaper than that for the outer solver. Throughout this study, r_2 is fixed to 0.9.

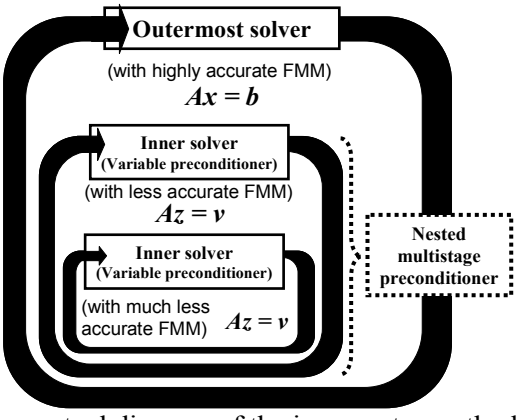

Figure 1: A conceptual diagram of the inner-outer methods.

3. Numerical Experience

In this section, we present numerical results to verify the accuracy and efficiency of the proposed implementation, and we conduct comparative experiments in respect of the strategies for the variable preconditioner. In the numerical experiments, we use FGMRES(m) for the outer and inner solvers and GMRES(m) for the innermost solver, with m representing the restart cycle.

The settings for the iterative solvers are summarized in Table 1. We investigate a total of 6 cases. All six cases are based on the proposed method and a policy of decreasing FMM accuracy down to the innermost solver. The far-field interaction is included with the truncation number determined by Eq. (8) for the 1st-level preconditioner, whereas no far-field interaction is considered for the 2nd-level one. The memory usage for FGMRES is twice that for standard GMRES for the same restart cycle, because FGMRES also stores the preconditioned Krylov basis vectors as well as the original Krylov basis. We therefore set the restart cycles for FGMRES and GMRES in such a way that all the cases have similar memory requirements.

In all the solvers for both the outer and inner iterations, the iteration process begins with the initial guess solution $\boldsymbol{x}_0 = \mathbf{0}$. The runs were carried out in double precision on the 16 AMD Opteron processors of an SGI Asterism server with 256 GB memory using OpenMP parallelization.

We consider a practical problem of a horn antenna radiating in the presence of a radome equipped with a frequency selective surface (FSS). Fiture 2 (a) displays the geometry of the antenna and the radome. The antenna is assumed to be a standard gain horn, which is modeled by specifying the aperture distribution of the electric and magnetic fields, with the dimensions of the aperture being 194 mm (x-axis) × 144 mm (y-axis). An FSS-embedded radome, having the shape of a partial sphere with a radius at the radome base of 12λ, is placed in front of the antenna aperture. The radome wall profile and the unit cell of the FSS layer are depicted in Figure 2(b) and (c). The dielectric layers are assumed to have the so-called "A-sandwich" structure, with two skin layers (ε_r = 4.277 and $\tan\delta$ = 1.695E-2) separated by a core layer (ε_r = 1.167 and $\tan\delta$ = 0.814E-2). As shown in Figure 2 (c), an FSS layer, which consists of a square-grid arrangement of ring-shaped slots on a conducting surface, is embedded in each of the two skin layers. We note that the configuration of this FSS radome is initially designed in a 2D planar model by evaluating the transmission and reflection properties, and the periodic arrangements of the unit cells are then mapped onto the spherical surfaces using a mapping scheme based on the geodesic. This geometry is discretized into 444,064 triangles, and the resultant linear system has 1,013,744 degrees of freedom. We use a denser mesh in this problem to capture the details of the equivalent currents, especially on the FSS layers. This test problem yields five levels for the MLFMA operator in the outer solver, with the truncation numbers being {9, 13, 20, 33, 58} for the free space of m = 1, {13, 20, 34, 60, 109} for the skin layer of m = 2, and {9, 13, 21, 35, 62} for the core layer of m = 3.

Table 3 tabulates the number of iterations, the CPU time required for convergence, and the memory usage for the CNs given in Table 1. CN 2 performs the best in terms of CPU time with some increase in the memory usage compared to the non-preconditioned case (CN 8). However, the impact of the memory increase is not significant considering the remarkable improvement in the convergence achieved by CN 2. We infer that we can effectively balance the CPU times consumed in the outer solver and the preconditioners by using a variable preconditioner with a moderately accurate FMM operator provided by Eq. (8) and a multistage preconditioner. Consequently, CN 2 is the preferred implementation from the viewpoint of both CPU time and memory requirements. The observations indicate that an FGMRES implementation, with a moderately accurate FMM operator in the inner solver and a multistage preconditioner with decreasing FMM accuracy down to the innermost solver, is the most prospective strategy for a problem with several levels of complexity.

Table 1: Settings for iterative solvers; CN ≡ case number, pre. ≡ preconditioner, sol. ≡ solver, itr. ≡ iteration, tol. ≡ tolerance.

CN		Max itr.	Tol.	Restart cycle	r_1	p
1	Outermost sol.	500	1.E-4	25	-	-
	1st-level pre.	20	0.3	20	0.5	0.2
	2nd-level pre.	10	0.1	10	0.0	0.0
2	Outermost sol.	500	1.E-4	25	-	-
	1st-level pre.	20	0.3	20	0.5	0.75
	2nd-level pre.	10	0.1	10	0.0	0.0
3	Outermost sol.	500	1.E-4	25	-	-
	1st-level pre.	20	0.3	20	0.5	0.95
	2nd-level pre.	10	0.1	10	0.0	0.0
4	Outermost sol.	500	1.E-4	25	-	-
	1st-level pre.	20	0.3	20	1.0	0.3
	2nd-level pre.	10	0.1	10	0.0	0.0
5	Outermost sol.	500	1.E-4	25	-	-
	1st-level pre.	20	0.3	20	1.0	0.55
	2nd-level pre.	10	0.1	10	0.0	0.0
6	Outermost sol.	500	1.E-4	25	-	-
	1st-level pre.	20	0.3	20	1.0	0.75
	2nd-level pre.	10	0.1	10	0.0	0.0
7	Outer solver	500	1.E-4	40	-	-
	Inner solver	20	0.3	20	0.0	0.0
8	Outer solver	5000	1.E-4	100	-	-
	Inner solver	-	-	-	-	-

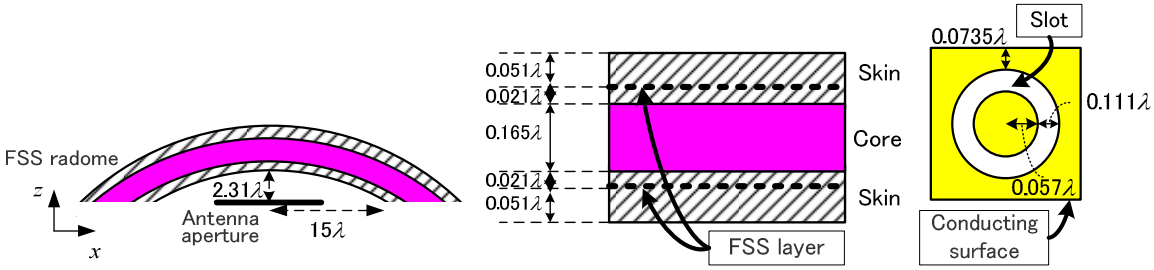

(a) Geometry of the antenna and the radome (b) FSS Radome wall profile (c) Unit cell of the FSS layer

Figure 2: Geometry of simulation model.

Figure: 3 A photograph of the fabricated FSS-embedded radome that was used for the measurement.

Table 2: Comparison of the number of iterations, CPU time, and memory usage.

CN	$L^i_{m,l}$ for the 1st-level preconditioner	Number of iterations	CPU time [s]	Memory usage [GB]
1	*m* =1: 4,4,5,6,6 *m* =2: 6,6,7,9,10 *m* =3: 4,4,5,6,6	29	306293.2	32.41
2	*m* =1: 4,6,11,19,32 *m* =2: 6,10,16,28,48 *m* =3: 4,6,11,19,32	12	167424.0	32.47
3	*m* =1: 4,7,14,28,55 *m* =2: 6,11,22,43,83 *m* =3: 4,7,14,28,55	12	194176.8	32.52
4	*m* =1: 9,10,11,13,15 *m* =2: 13,14,17,19,22 *m* =3: 9,10,11,13,15	13	197612.1	32.03
5	*m* =1: 9,13,19,28,41 *m* =2: 13,19,27,40,59 *m* =3: 9,13,19,28,41	11	179702.4	32.10
6	*m* =1: 9,11,18,29,52 *m* =2: 13,18,30,54,104 *m* =3: 9,11,18,31,55	11	170432.5	32.16
7	*m =1, 2, 3: 0,0,0,0,0,0*	148	309048.3	31.80
8	-	2163	534216.3	31.73

4. Conclusions

In this paper, we have proposed a method to accelerate the FGMRES based on the MoM and FMM techniques. We have reconsidered the definition of the truncation number in the inner solver and extended it to an implementation based on the CTF for electromagnetic scattering and radiation problems with composite dielectric and conducting objects. The numerical experiments revealed that, similar to the VSIE formulation given in Ref. [2], a moderately accurate FMM operator provides the optimal preconditioner. Furthermore, we investigated the effectiveness of a multistage preconditioner by applying the inner-outer concept recursively. We observed that our new FGMRES implementation strikes a balance between the CPU time and the memory requirements. As a consequence, it is a promising strategy for solving large-scale and practical scattering and radiation problems.

Acknowledgments

This study has been conducted in the context of a project entitled "Development of Advanced Aircraft System Technology (Development of Advanced Material Technology for Airborne System)" which is supported by Ministry of Economy, Trade and Industry.

References

[1] Y. Saad, “A flexible inner-outer preconditioned GMRES algorithm,” SIAM J. Sci. Comput., vol. 14, no. 2, pp. 461–469, Mar. 1993.

[2] H. Chiba, T. Fukasawa, H. Miyashita, and Y. Konishi, “Efficient implementation of inner-outer flexible GMRES for the method of moments based on a volume-surface integral equation,” IEICE Trans. Electron., vol. E94-C, no. 1, pp. 24–31, Jan. 2011.

[3] P. Ylä-Oijala, M. Taskinen, and S. Järvenpää, “Surface integral equation formulations for solving electromagnetic scattering problems with iterative methods,” Radio Sci., vol. 40, Nov. 2005, RS6002, doi:10. 1029/2004RS003169.

[4] W. C. Chew, J.-M. Jin, E. Michielssen, and J. M. Song, eds., Fast and Efficient Algorithms in Computational Electromagnetics. Boston-London: Artech House Publishers, 2001.

[5] Z. H. Fan, R. S. Chen, E. K. N. Yung, and D. X. Wang, “Inner-outer GMRES algorithm for MLFMA implementation,” 2005 IEEE Antennas and Propagation Soc. Int. Symp. Digest, vol. 4A, pp 463–466, July 2005.